Electronic Supplementary Material (ESI) for Physical Chemistry Chemical Physics.

Supporting Information

Structural and functional role of anions in electrochemical water oxidation probed by arsenate incorporation into cobalt-oxide materials

Javier Villalobos, Diego González-Flores*, Katharina Klingan, Petko Chernev, Paul Kubella, Roberto Urcuyo, Chiara Pasquini, Mohammad Reza Mohammadi, Rodney D.L. Smith, Mavis L. Montero* and Holger Dau*

Experimental methods

SEM analysis. Sample morphology and constituent elements were determined through a Low Vacuum Scanning Electron Microscope, HITACHI S-3700N, equipped with an energy dispersive X-ray analysis probe, Oxford (EDS) and a Hitachi S-570 with an Aspe model Sirius 10/7.5 EDS.

IR Spectra. ATR-FTIR was performed in a Thermo Scientific Nicolet 6700 in ATR mode using a diamond crystal.

UV-visible. Measurements were performed with a Lambda 1050 Spectrophotometer UV-VIS-NIR.

X-ray diffraction. XRD was performed on a Bruker AXS-D8 Advance with a copper X-ray tube using Göbel mirror and a Lynx-Eye detector. Locked coupled was used from 2Θ = 10° to 70° on increments of 0.019° and an equivalent time of 768 s per step.

TXRF measurements. Elemental analysis was done using a PicoFox Spectrometer (Bruker) for total reflection X-ray fluorescence (TXRF) measurements. For quantification the sample deposited on the electrodes was dissolved in 500 µl of 30% HCl by exposing the films to the acid for several minutes. After dissolution, 500 µL of a Ga standard ($Ga(NO_3)_3$, concentration of 10 mg/L) was added and 5 µL of the mixture were deposited on a silicon-coated quartz glass sample plate. The XRF acquisition time was 30 min per sample.

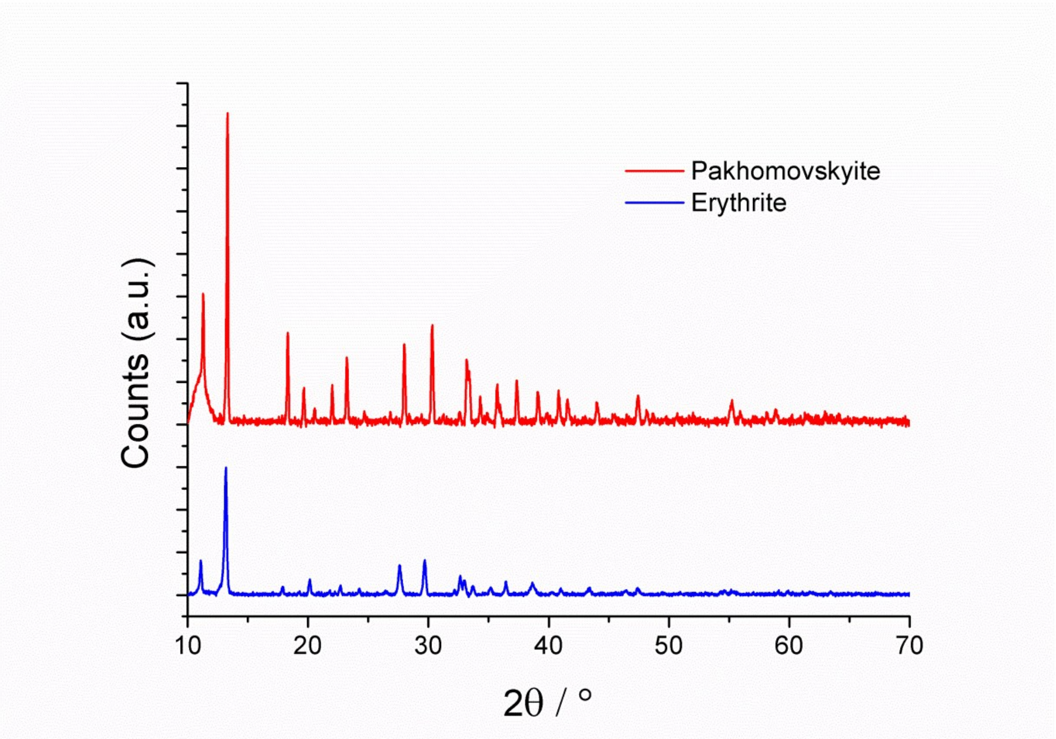

Figure S1. Powder X-ray diffractograms for pakhomovskyite and erythrite. Peak positions confirm that both mineral phases were synthesized successfully.

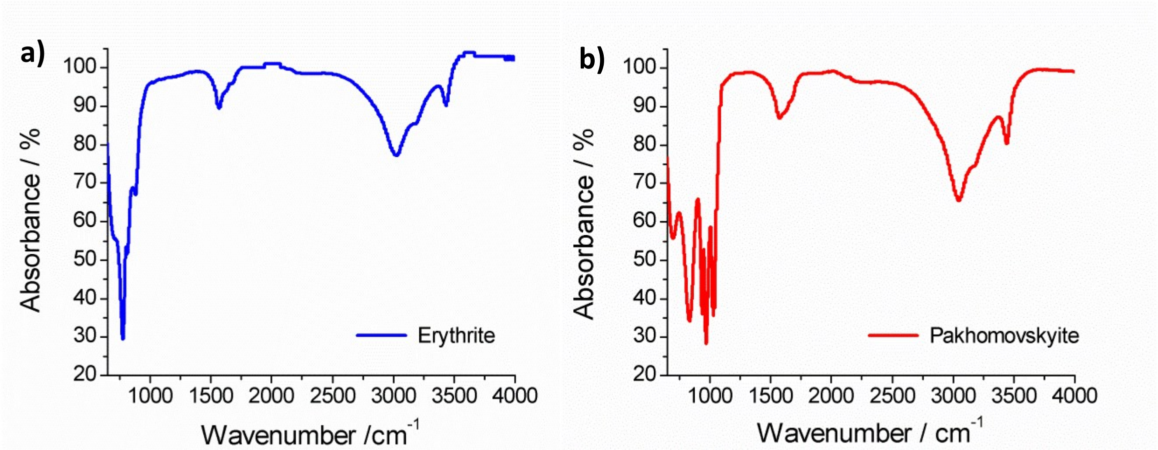

Figure S2. ATR-FTIR spectra for (a) erythrite and (b) pakhomovskyite.

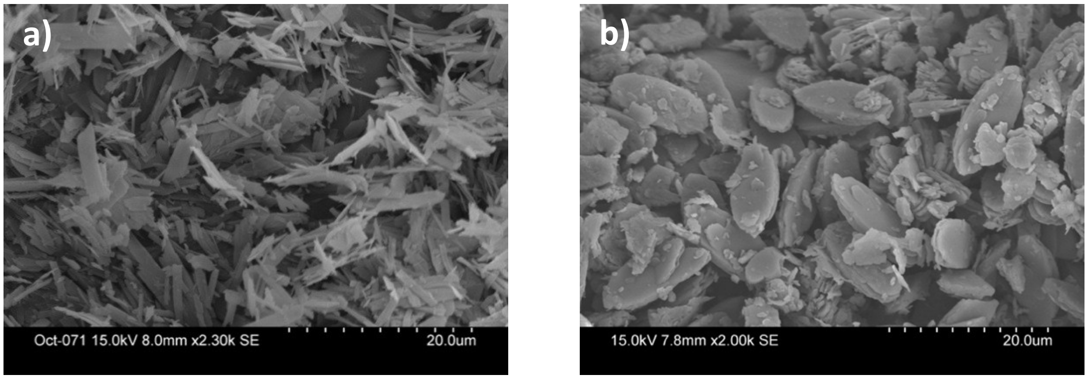

Figure S3. SEM images for erythrite (a) and pakhomovskyite (b) powders.

Table S1. BET surface area analysis for erythrite and pakhomovskyite powders.

Measured property	**Erythrite**	**Pakhomovskyite**
Surface area, BET ($m^2\ g^{-1}$)	20.9 ± 0.3	13.9 ± 0.1
Surface area, Langmuir ($m^2\ g^{-1}$)	33.4 ± 0.4	23.0 ± 0.6
External surface area ($m^2\ g^{-1}$)	29.0	20.7

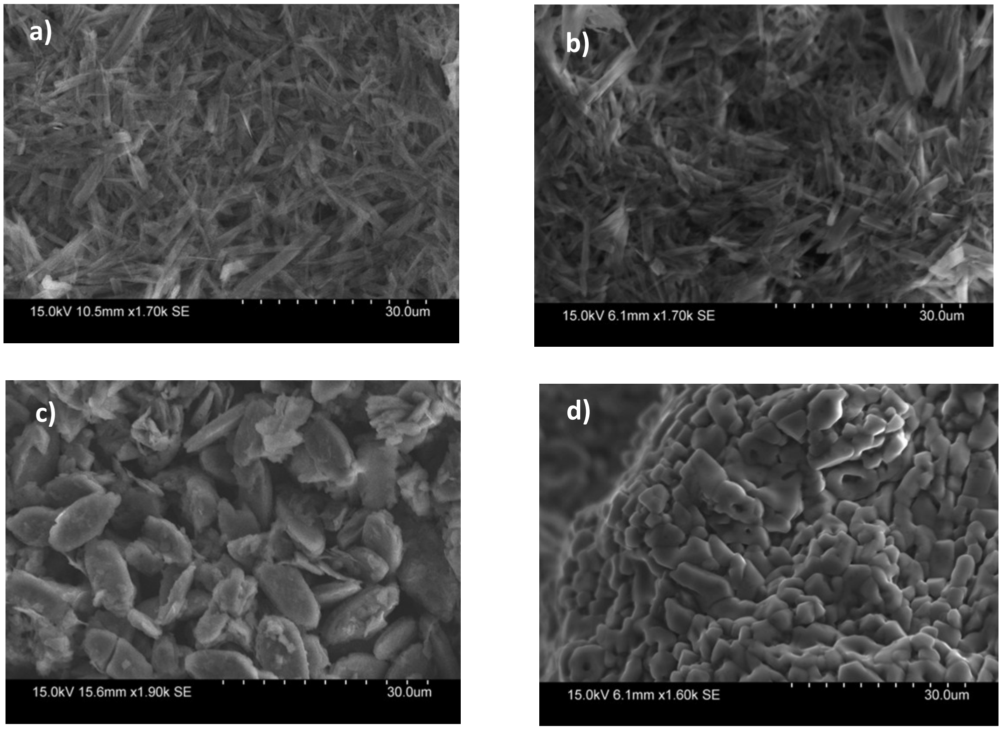

Figure S4. SEM images for both compounds immobilized on FTO substrates, before and after 200 CV cycles. (**a**) erythrite. (**b**) erythrite after 200 cycles. (**c**) pakhomovskyite. (**d**) pakhomovskyite after 200 cycles. CV measurements were performed with 100 mV s^{-1} in 0.1 M phosphate buffer at pH 7.

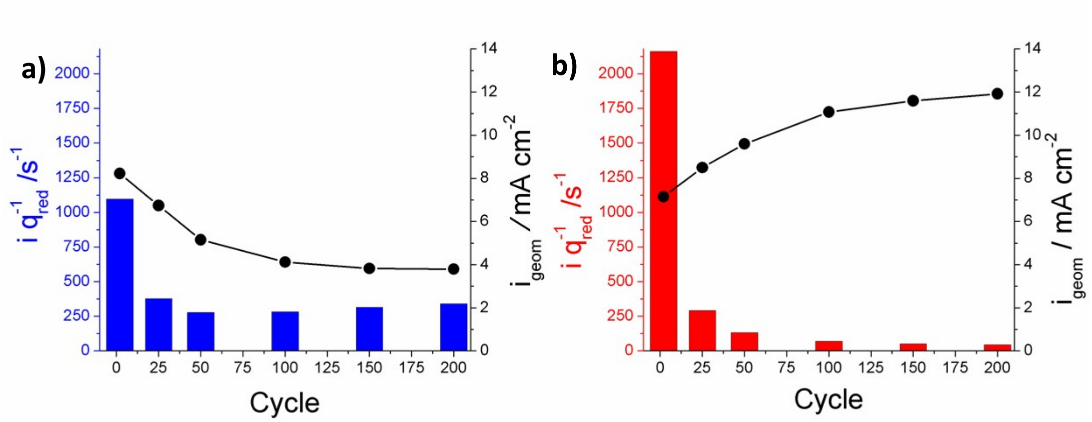

Figure S5. Catalytic current (i_{geom}) and TOF per redox-active site (i q_{red}^{-1}) versus the number of CV cycles, during OER for **a)** erythrite and **b)** pakhomovskyite. Redox charge (q_{red}) was calculated by integration of the reductive currents of the CV shown in Figure S10. Catalytic activity was estimated from the maximal current density measured in the respective cycle (at 2.12 V vs RHE) and is indicated by black circles (right y-axis). Bars indicate the ratio between maximal current density (i_{geom}) and redox charge (q_{red}) in units of s^{-1} (left y-axis). All data is given in respect to the geometrical electrode area (1 cm²).

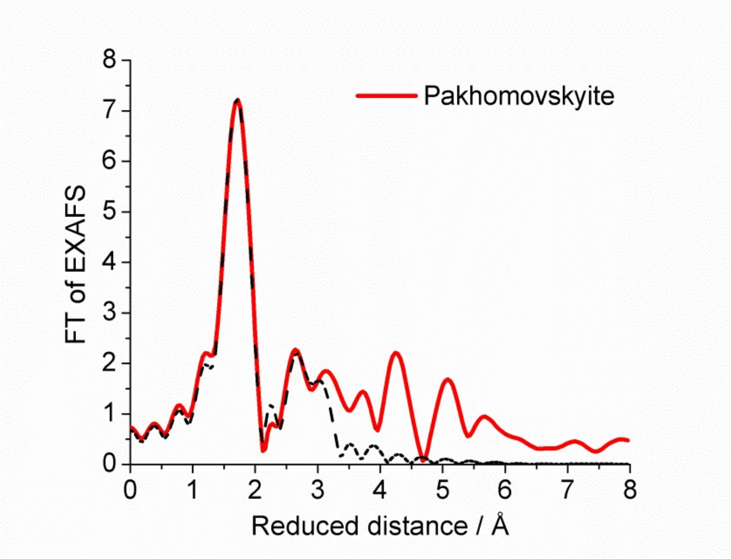

Figure S6. Fourier-transformed EXAFS of pakhomovskyite powder at the Co K-edge. The dotted line results from EXAFS simulations (see Table S2 for parameters).

Table S2. Parameters obtained by simulation of the k^3-weighted EXAFS spectra for cobalt K-edge in pakhomovskyite powder. The simulated spectra correspond to the Fourier-transformed EXAFS spectra shown in Figure S6. The errors represent the 68% confidence interval of the respective fit parameter (N; coordination number, R; absorber-backscatter distance, and σ; EXAFS Debye–Waller parameter). The numbers in parentheses correspond to the uncertainty in the last digit.

	Co-O	**Co-Co**	**Co-P**	**Co-P**	**Co-O**
R [Å]	2.06(1)	2.94(3)	3.23(4)	3.36(6)	3.48(7)
N	6*	0.67*	2*	1.33*	2*
σ [Å]	0.063(4)	0.0707*	0.0707*	0.0707*	0.0707*

*Represents the parameters that are fixed during the simulation. The coordination numbers were fixed according to the crystal structure.

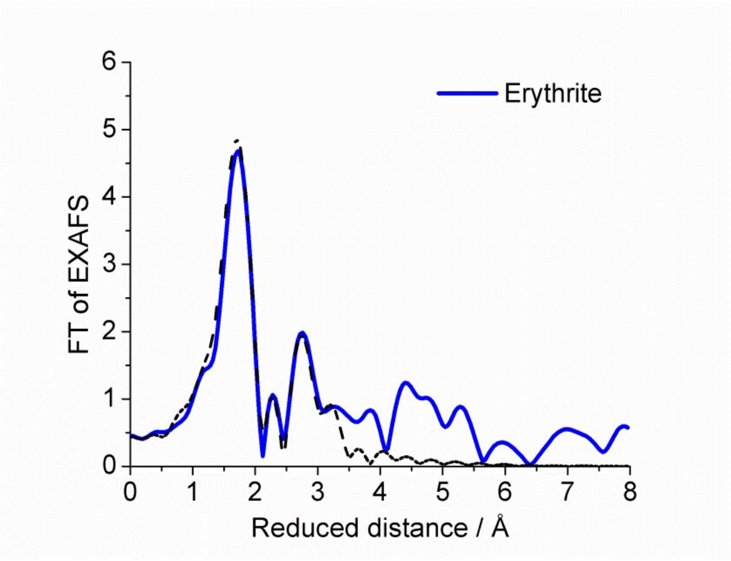

Figure S7. Fourier-transformed EXAFS of erythrite powder at the Co K-edge. The dotted line results from EXAFS simulations (see Table S3 for parameters).

Table S3. Parameters obtained by simulation of the k^3-weighted EXAFS spectra for cobalt K-edge in Erythrite powder. The simulated spectra correspond to the Fourier-transformed EXAFS spectra shown in Figure S7. The errors represent the 68% confidence interval of the respective fit parameter (N; coordination number, R; absorber-backscatter distance and σ; EXAFS Debye–Waller parameter). The numbers in parentheses correspond to the uncertainty in the last digit.

	Co-O	**Co-Co**	**Co-As**	**Co-As**	**Co-O**
R [Å]	2.09(1)	3.05(3)	3.26(3)	3.40(7)	3.6(1)
N	6*	0.67*	2*	1.33*	2*
σ [Å]	0.086(5)	0.0707*	0.0707*	0.0707*	0.0707*

*Represents the parameters that are fixed during the simulation. The coordination numbers were fixed according to the crystal structure.

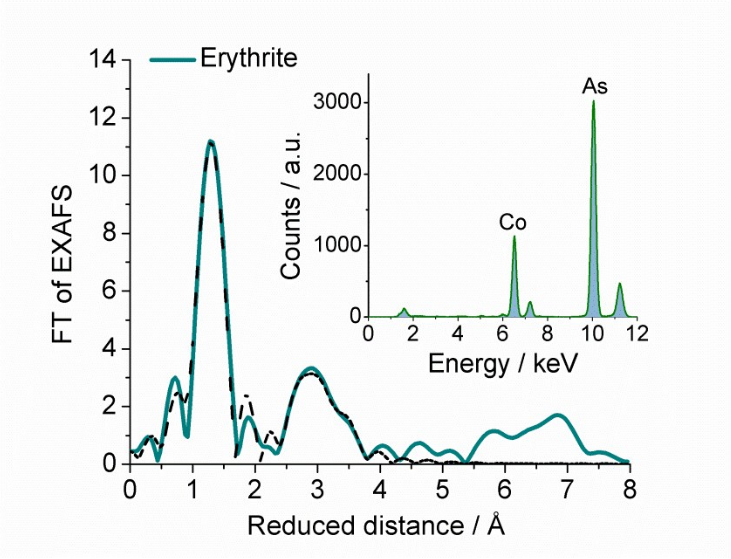

Figure S8. Fourier-transformed EXAFS of erythrite powder at the As K-edge. The simulation of the data is shown by the dotted line (see Table S4 for parameters). The inset shows the fluorescence emission spectrum with the energy of the incoming X-ray beam at 11900 eV, the arsenic and cobalt K_α peaks are indicated.

Table S4. Parameters obtained by simulation of the k^3-weighted EXAFS spectra for arsenic K-edge in erythrite powder. The simulated spectra correspond to the Fourier-transformed EXAFS spectra shown in Figure S8. The errors represent the 68% confidence interval of the respective fit parameter (*N*; coordination number, *R*; absorber-backscatter distance, and σ; EXAFS Debye–Waller parameter). The numbers in parentheses correspond to the uncertainty in the last digit.

	As-O	**As-O**	**As-Co**	**As-O**	**As-Co**	**As-O**	**As-As**
R [Å]	1.68(1)	2.92(7)	3.27(2)	3.4(2)	3.42(4)	3.4(1)	3.67(3)
N	3.8(2)*	1*	3*	2*	2*	3*	1*
s [Å]	0.0524*	0.0592*	0.0592*	0.0592*	0.0592*	0.0592*	0.0592*

*Represents the parameters that are fixed during the simulation. The coordination numbers were fixed according to the crystal structure.

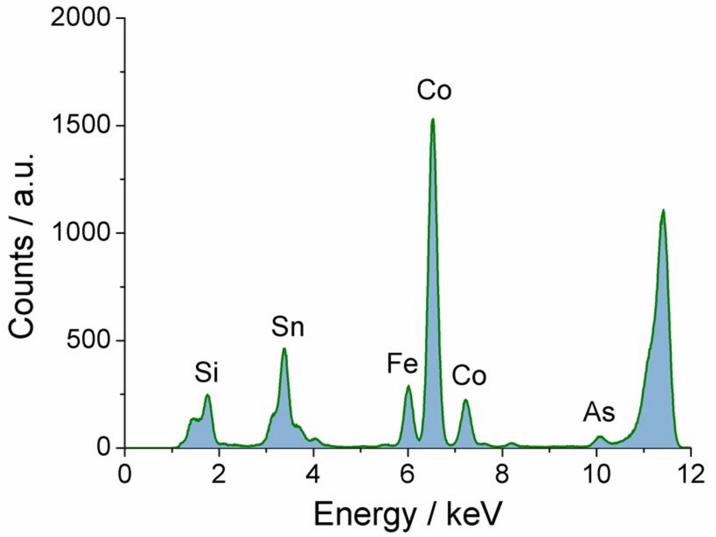

Figure S9. Fluorescence emission spectrum for erythrite amorphized in phosphate (800 cycles 0.05 M and pH 7 phosphate buffer) with the energy of the incoming X-ray beam at 11900 eV. The arsenic and cobalt K_α peaks are indicated.

Electrochemical characterization by cyclic voltammetry

The evaluation of the redox and catalytic properties of **Pak** and **Ery** was performed by cyclic voltammetry (CV) measurements (in phosphate buffer at pH 7). In this case we used a wider potential range and higher scan rate than in previously reported work[1] (Figure S10). Both compounds have a similar maximum current density of around 7-8 mA cm^{-2} in the first cycle (CVs in Figure S10). The similar initial catalytic current density for both minerals fits well to the similar BET (Brunauer-Emmet-Teller) surface areas (values given in Table S1). **Pak** shows a higher increase in redox area during continuous cycling in phosphate buffer than **Ery.** This difference is related to the faster amorphization process of **Pak** compared with **Ery**, and to a higher stability of **Ery** towards amorphization. Figure S5 shows a comparison between TOF (turnover frequency) values (calculated per Co ions present in the catalyst and evolved O_2 molecule) for both catalysts. The catalytic TOF of **Ery** is decreased by a factor of 5 and by a factor of 100 for **Pak,** both during 200 CV. However, stability properties of **Pak** and **Ery** are beyond the scope of the present work and will be presented in a follow-up publication.

Amorphization of the **Ery** mineral cannot be completed under these conditions, and requires a modified electrochemical protocol of 800 cycles and a lower phosphate buffer concentration of 0.05 M (Figure S10c and S11). These optimized protocols provided a better signal to noise ratio than our previous work (Figure S7 and S12)[1].

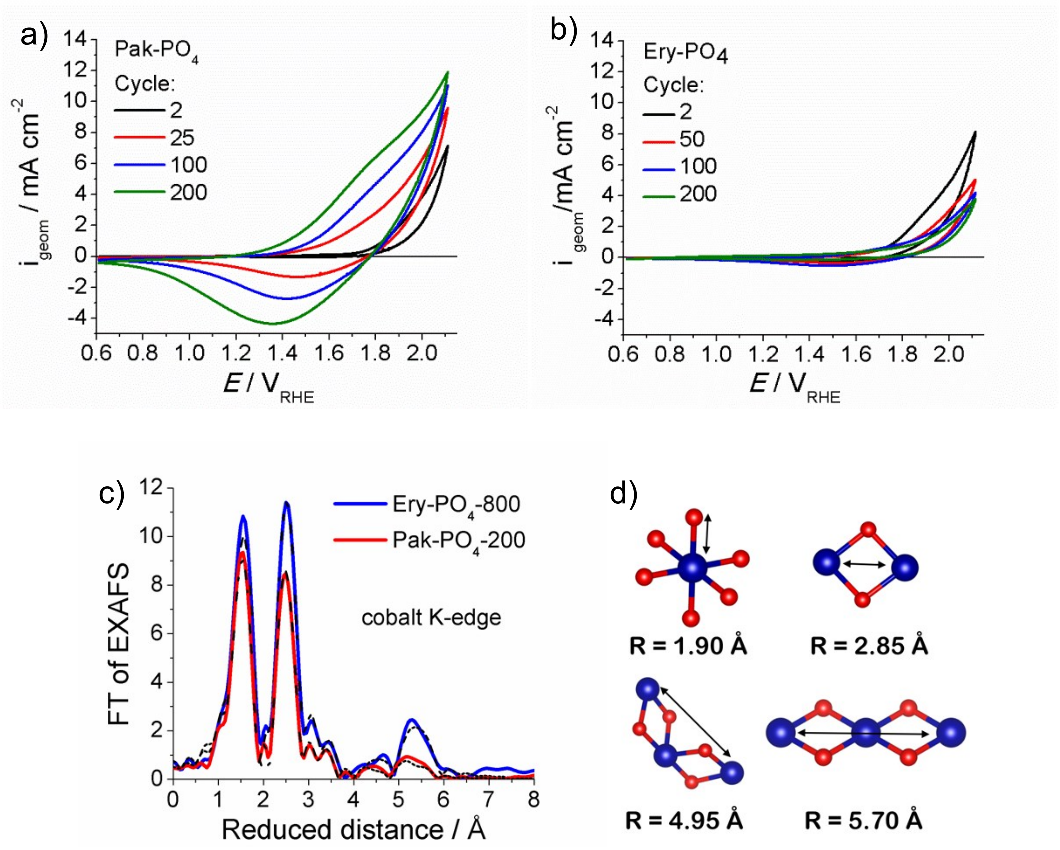

Figure S10. Series of CV for: (**a**). **Pak** measured in phosphate buffer (Pak-PO$_4$). (**b**). **Ery** measured in phosphate buffer (Ery-PO$_4$). (E vs. RHE; CV with 100 mVs^{-1} in 0.1 M phosphate buffer at pH 7, 85 % IR compensation). (**c**). Fourier-transform EXAFS spectra collected at the cobalt K-edge for **Pak** (red line) and **Ery** (blue line) deposited on FTO electrodes. Pak-PO$_4$ amorphization was obtained after 200 CV cycles (100 mVs^{-1} in 0.1 M phosphate buffer at pH 7); Ery-PO$_4$ amorphization was obtained after 800 CV cycles (100 mVs^{-1} in 0.05 M phosphate buffer at pH 7). The indicated reduced distance is by about 0.4 Å shorter than the precise distance obtained by EXAFS simulations. The dotted lines results from EXAFS simulations (see Table S5 for parameters). (**d**). Structural motifs and reported distances, R, for cobalt oxide. Blue balls represent cobalt atoms and red balls oxygen atoms.

Table S5. EXAFS absorber-backscatter distance, *R*, and coordination numbers, *N*, as determined from simulation of the k^3-weighted EXAFS spectra at the cobalt K-edge for Pakhomovskyite and erythrite amorphized in phosphate (samples Pak-PO_4 and Ery-PO_4).

	Co-O	**Co-O**	**Co-Co/As**	**Co-X**[a]	**Co-Z**[b]	**Co-Co**	**Co-Co**	**Co-Co**
Pak-PO_4 cobalt K-edge								
R [Å]	1.90(1)	2.21(3)	2.81(1)	3.21(2)	3.71(4)	4.95(4)	5.15(4)	5.63(1) *
N	5.5(3)	1.0(4)	3.9(2)	1.8(5)	0.5(4)	2(1)	2(1)	0.7(5)
Ery-PO_4 cobalt K-edge								
R [Å]	1.91(1)	2.2(3)	2.85(1)	3.08(1)	3.81(4)	5.01(3)	5.22(3)	5.70(1) *
N	5.8(2)	0.2(2)	6.3(4)	2.6(6)	1.0(6)	4(1)	4(2)	2.2(6)

[a, b] Shells were simulated with Co-Co phase functions.

.* This distance was set as twice the 2.81-2.85 Å Co-Co distance and simulated using multiple scattering as in ref.[2] The Debye-Waller factor, σ, was set to 0.071 for all simulations. The numbers in parenthesis correspond to the likely error in the last digit (1 σ error range).

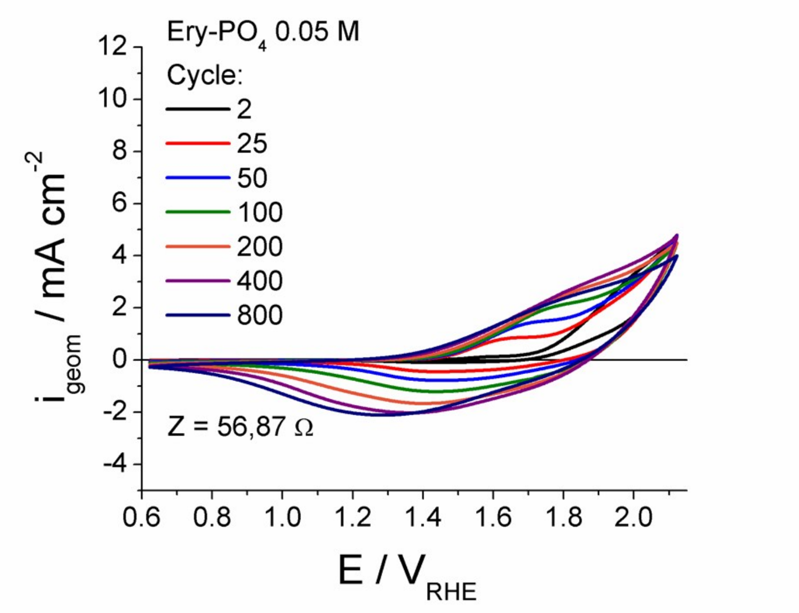

Figure S11. Erythrite amorphized in phosphate buffer (Ery-PO_4). The sample was deposited on FTO electrodes. The amorphization was obtained after 800 CV cycles (100 mVs^{-1} in 0.05 M phosphate buffer at pH 7). Z represents the buffer electrical resistance.

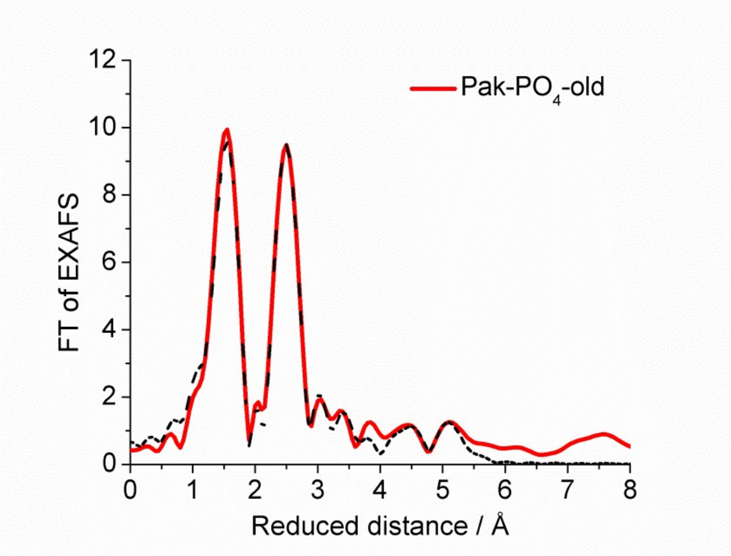

Figure S12. Fourier-transformed EXAFS of pakhomovskyite after amorphization in phosphate buffer at the Co K-edge. The sample corresponds to the sample A measured in reference[1] that was amorphized under a different protocol. For the amorphization the sample was exposed to 200 cycles with 10 mV s^{-1} in 0.1 M phosphate between 1.11 V and 1.86 V versus RHE. The dotted line results from EXAFS simulations (see Table S6 for parameters).

Table S6. Parameters obtained by simulation of the k^3-weighted EXAFS spectra for cobalt K-edge in pakhomovskyite after amorphization in phosphate buffer. The simulated spectra correspond to the Fourier-transformed EXAFS spectra shown in Figure S12. The errors represent the 68% confidence interval of the respective fit parameter (*N*; coordination number, *R*; absorber-backscatter distance). The numbers in parentheses correspond to the uncertainty in the last digit.

	Co-O	**Co-O**	**Co-Co**	**Co-X**[a]	**Co-Z**[b]	**Co-Co**	**Co-Co**	**Co-Co**
R [Å]	1.90(1)	2.20(4)	2.83(1)	3.04(1)	3.71(6)	4.90(3)	5.10(3)	5.65(1)*
N	5.7(4)	0.9(6)	5.2(4)	2.2(6)	0.5(5)	4(2)	4(2)	0.5(7)

[a]This shell was simulated as a Co-Co distance

[b]A Co-Co phase functions was used for EXAFS simulation of this shell.

.* This distance was set as twice the 2.81-2.85 Å Co-Co distance and simulated using multiple scattering as in ref. [2]

σ, was set to 0.071 for all simulations. The numbers in parenthesis correspond to the likely error in the last digit (1 σ error range)

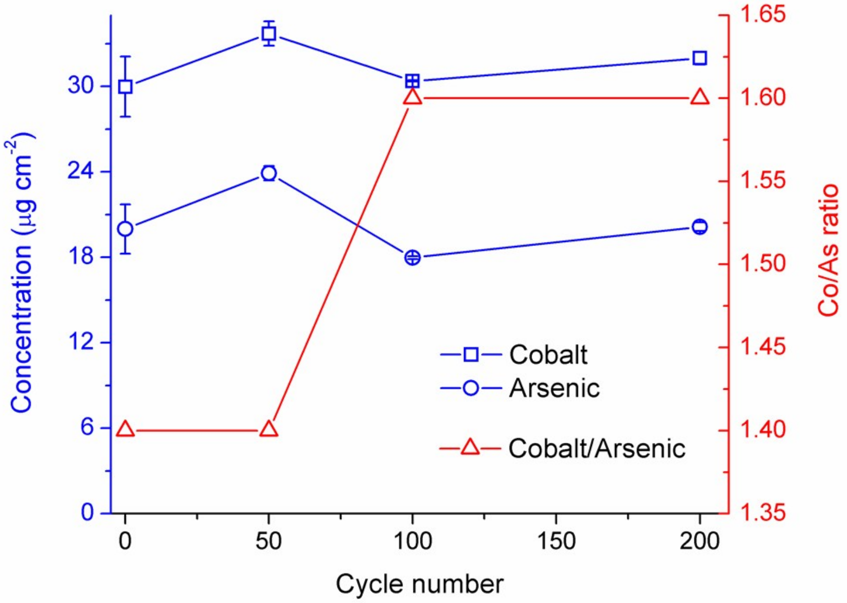

Figure S13. Quantification of cobalt and arsenic concentration in erythrite electrodes after 0, 50, 100 and 200 cycles in phosphate buffer pH 7 and 0.1 mol L^{-1}. Catalysts were immobilized on FTO electrodes, exposed to a number of certain CV cycles, then washed and dissolved in 1 mL of 30 % HCl. The quantification was performed by TXRF as described in the experimental section.

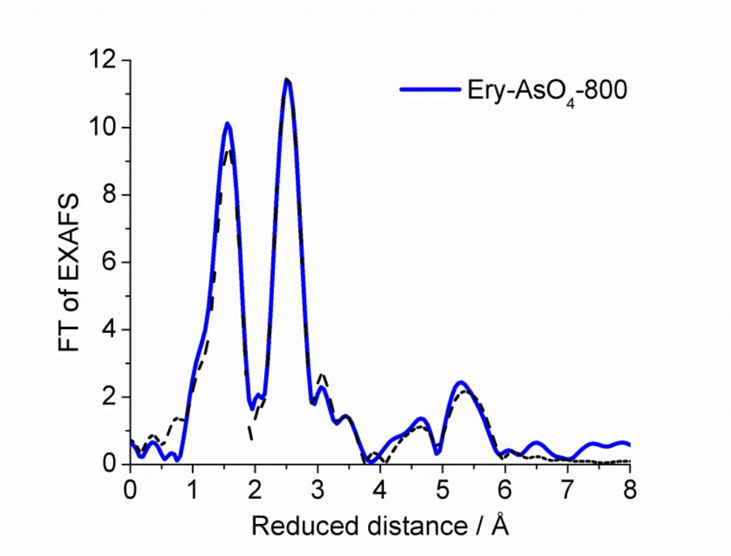

Figure S14. Fourier-transformed EXAFS of erythrite after amorphization in arsenate buffer at the Co K-edge. For the amorphization the sample was exposed to 800 cycles with 100 mVs^{-1} in 0.05 M and pH 7 arsenate buffer. The dotted line results from EXAFS simulations (see Table S7 for parameters).

Table S7. Parameters obtained by simulation of the k^3-weighted EXAFS spectra for cobalt K-edge of erythrite after amorphization in arsenate buffer. The simulated spectra correspond to the Fourier-transformed EXAFS spectra shown in Figure S14. The errors represent the 68% confidence interval of the respective fit parameter (*N*; coordination number, *R*; absorber-backscatter distance). The numbers in parentheses correspond to the uncertainty in the last digit.

	Co-O	**Co-O**	**Co-Co**	**Co-X**[a]	**Co-Z**[b]	**Co-Co**	**Co-Co**	**Co-Co**
R [Å]	1.91(1)	2.2(1)	2.85(1)	3.08(2)	3.81(5)	5.00(3)	5.22(4)	5.71(1)*
N	5.6(3)	0.5(3)*	6.5(6)	2.7(7)	0.9(7)	4(2)	4(3)	2.1(8)

[a] This shell was simulated as a Co-Co distance

[b] A Co-Co phase functions was used for EXAFS simulation of this shell.

.* This distance was set as twice the 2.81-2.85 Å Co-Co distance and simulated using multiple scattering as in ref. [2]

σ, was set to 0.071 for all simulations. The numbers in parenthesis correspond to the likely error in the last digit (1 σ error range)

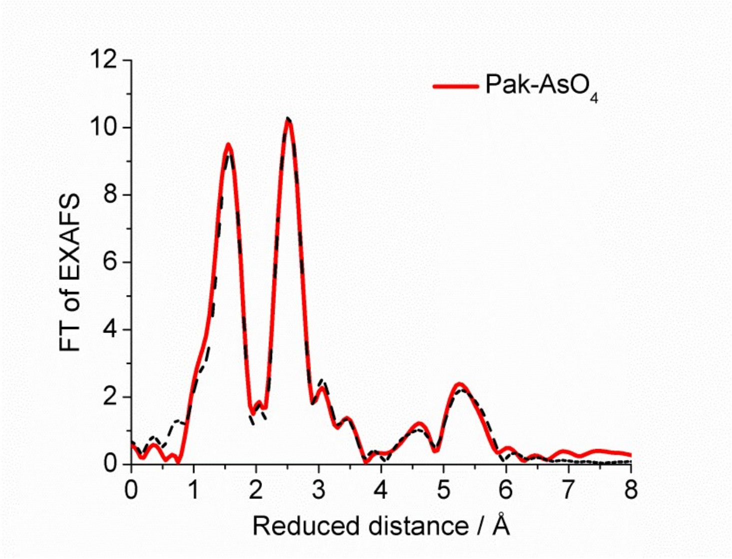

Figure S15. Fourier-transformed EXAFS of pakhomovskyite after amorphization in arsenate buffer at the Co K-edge. For the amorphization the sample was exposed to 200 cycles with 100 mVs^{-1} in 0.1 M and pH 7 arsenate buffer. The dotted line results from EXAFS simulations (see Table S8 for parameters).

Table S8. Parameters obtained by simulation of the k^3-weighted EXAFS spectra for cobalt K-edge of pakhomovskyite after amorphization in arsenate buffer. The simulated spectra correspond to the Fourier-transformed EXAFS spectra shown in Figure S15. The errors represent the 68% confidence interval of the respective fit parameter (*N*; coordination number, *R*; absorber-backscatter distance). The numbers in parentheses correspond to the uncertainty in the last digit.

	Co-O	**Co-O**	**Co-Co**	**Co-X[a]**	**Co-Z[b]**	**Co-Co**	**Co-Co**	**Co-Co**
R [Å]	1.92(1)	2.23(3)	2.86(1)	3.09(1)	3.81(4)	4.99(2)	5.20(2)	5.71(1)*
N	5.7(3)	1.2(4)	5.7(4)	2.5(4)	0.7(5)	4(2)	5(2)	1.9(5)

[a] This shell was simulated as a Co-Co distance

[b] A Co-Co phase functions was used for EXAFS simulation of this shell.

.* This distance was set as twice the 2.81-2.85 Å Co-Co distance and simulated using multiple scattering as in ref. [2]

σ, was set to 0.071 for all simulations. The numbers in parenthesis correspond to the likely error in the last digit (1 σ error range)

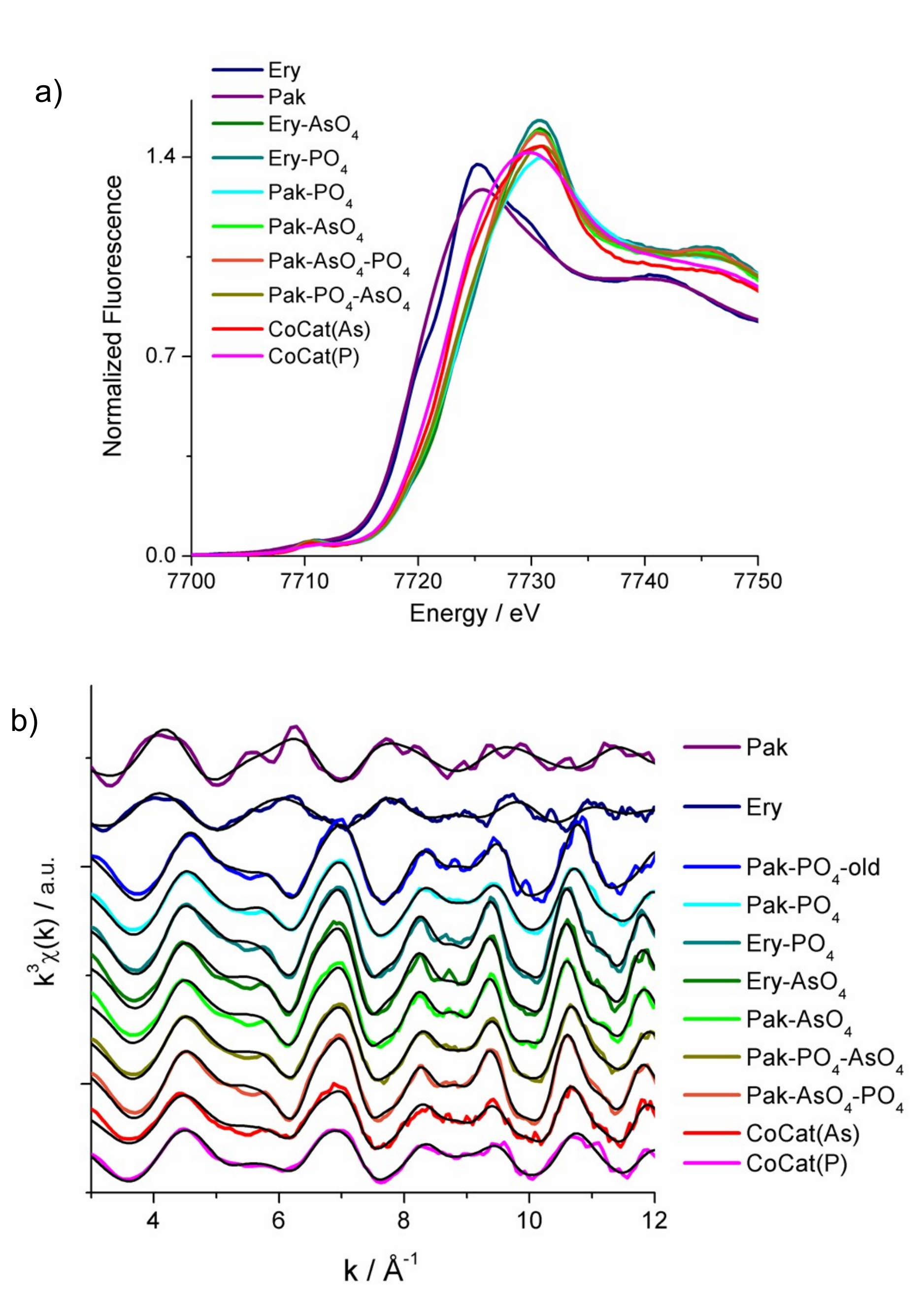

Figure S16. a**)** XANES spectrum of different catalysts at the cobalt K-edge. In all cases catalysts after amorphization showed and oxidation state close to 3.b) K^3-weighted EXAFS spectra of catalysts recorded at the K-edge of cobalt. The black lines represent the respective EXAFS simulations. **Pak**: pakhomovskyite powder; **Ery**: erythrite powder; **Pak-PO$_4$-old**: pakhomovskyite amorphized with the previous protocol in phosphate buffer; **Pak-PO$_4$**: pakhomovskyite amorphized in phosphate; **Ery-PO$_4$**: erythrite amorphized in phosphate; **Ery-AsO$_4$**: erythrite amorphized in arsenate; **Pak-AsO$_4$**: pakhomovskyite amorphized in arsenate; **Pak-PO$_4$-AsO$_4$**: pakhomovskyite amorphized in phosphate and exchanged in arsenate; **Pak-AsO$_4$-PO$_4$**: pakhomovskyite amorphized in arsenate and exchanged in phosphate; **CoCat(As)**: CoCat deposited in arsenate buffer.

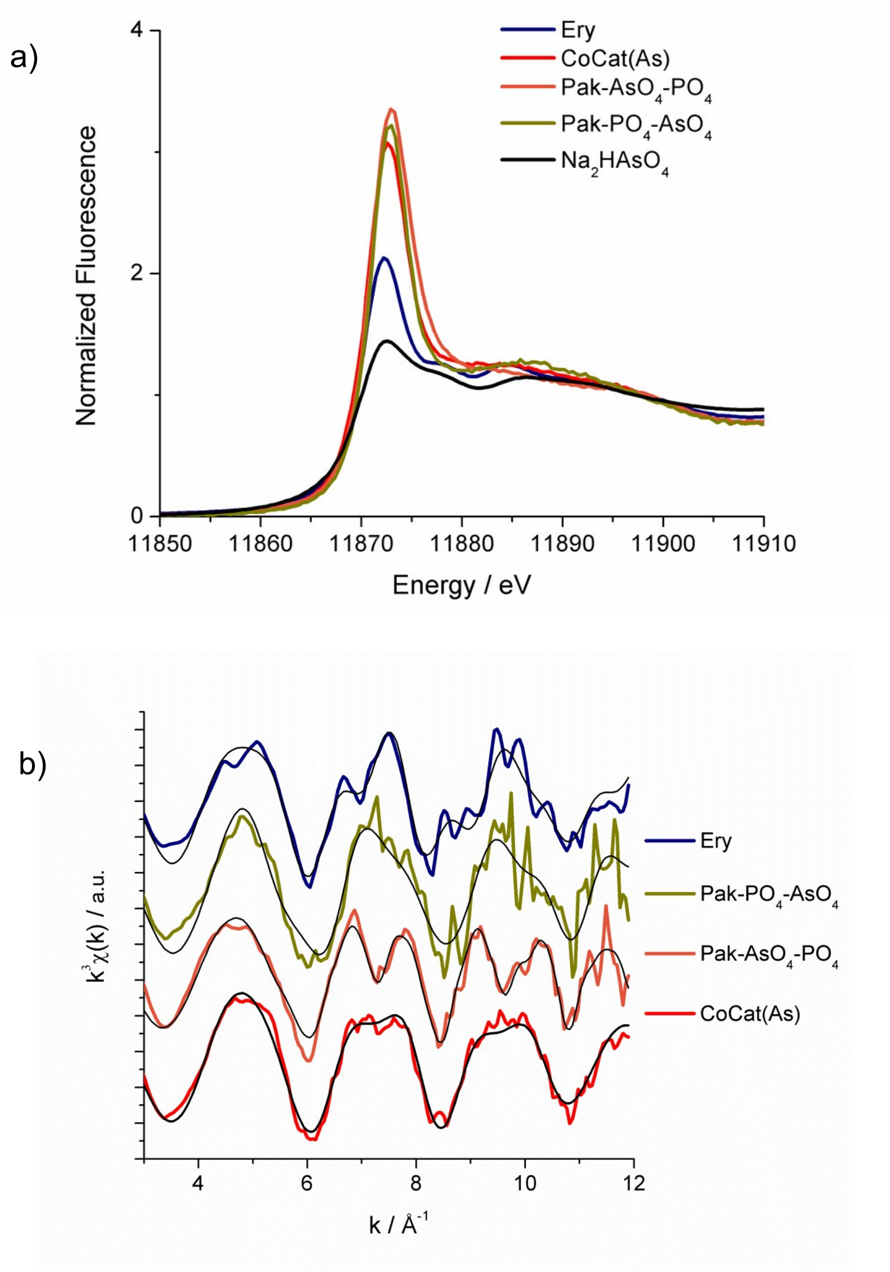

Figure S17. a) XANES spectrum of different catalysts at the arsenic K-edge. All measured samples are consistent with arsenic in oxidation state +5.[3] An increase in the absorption maximum was observed for amorphous samples, which suggests a change in the coordination environment in comparison to the erythrite sample. **b)** K^3-weighted EXAFS spectra of catalysts recorded at the K-edge of arsenic. The black lines represent the respective EXAFS simulations. **Ery**: erythrite powder; **Pak-PO4-AsO4**: pakhomovskyite amorphized in phosphate and exchanged in arsenate; **Pak-AsO4-PO4**: pakhomovskyite amorphized in arsenate and exchanged in phosphate; **CoCat(As)**: CoCat deposited in arsenate buffer.

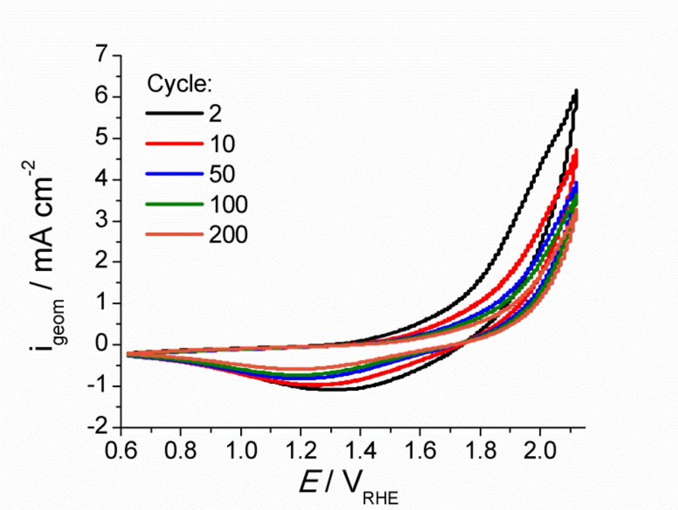

Figure S18. Series of CV for arsenate (0.1 M and pH 7) anionic exchange in amorphized pakhomovskyite. Prior to the anionic exchange the pakhomovskyite was amorphized in 0.1 M phosphate buffer pH 7 (Figure S10). After the amorphization in phosphate buffer, the electrolyte is exchanged to arsenate buffer (0.1 M, pH 7) and CV measurements are performed for 200 cycles with 85 % iR compensation.

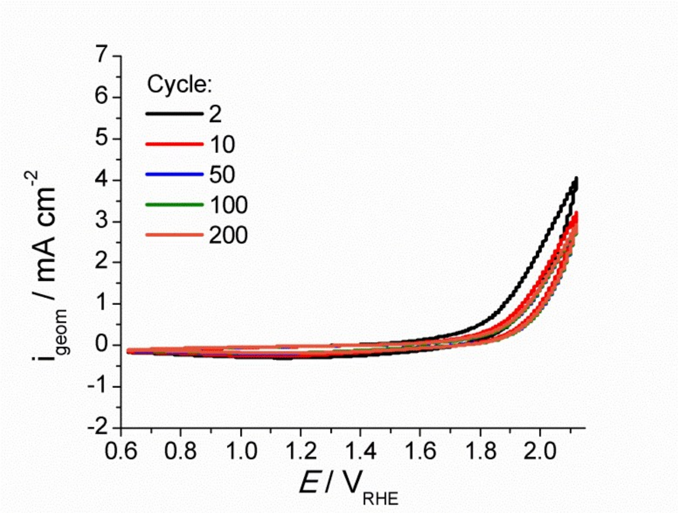

Figure S19. Series of CV for phosphate (0.1 M and pH 7) anionic exchange in amorphized pakhomovskyite. Prior to the anionic exchange the pakhomovskyite was amorphized in 0.1 M arsenate buffer pH 7 (Figure S10). After the amorphization in arsenate buffer the electrolyte is exchanged to phosphate buffer (0.1 M and pH 7) and CV measurements are performed for 200 cycles with 85 % iR compensation.

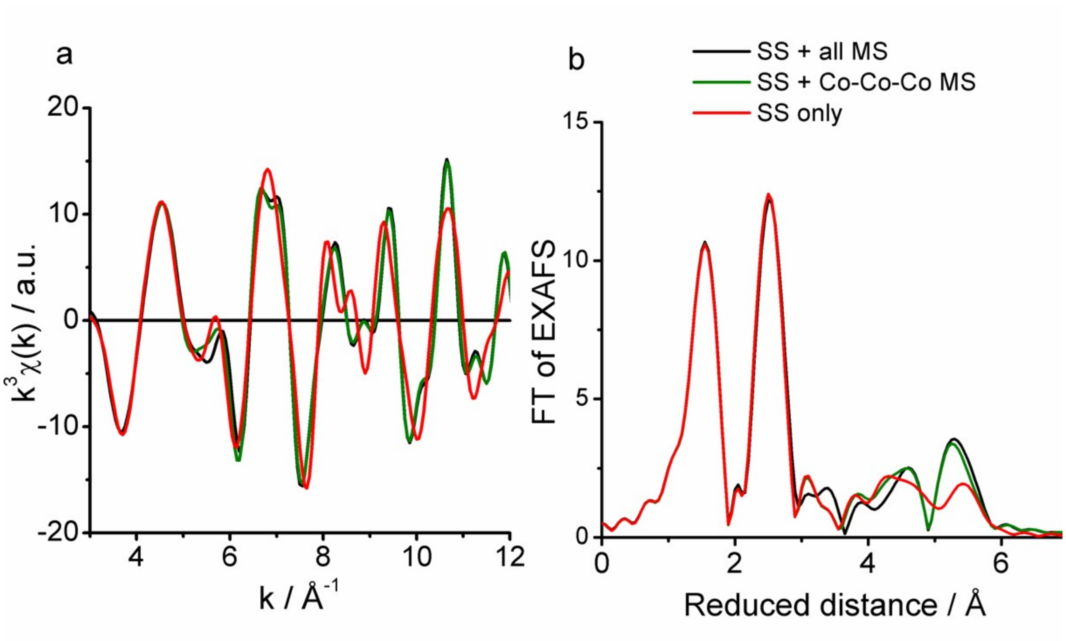

Figure S20. FEFF simulation of Co K-edge k^3-weighted EXAFS (left) and its Fourier-transform (right) of a model similar to the one shown in Figure 4 in the main text. Black line: all single- and multiple-scattering paths included (44 shells); green line: all single-scattering plus multiple-scattering from co-linear Co-Co-Co motifs (14 shells), corresponding to the fitting approach in this work; red line: only single-scattering paths (12 shells) included. Debye-Waller factor, σ, was set to 0.071 for all shells; paths with a maximum of 6 legs up to 7 Å were considered; self-consistent field option in FEFF was on. We note that omitting most multiple-scattering paths (green line) results in a simulation that is very similar to the complete simulation (black line), with effects limited to the 3-4.5 Å reduced distance range; for an amorphous structure with variations of bond angles these effects would be presumably further decreased.

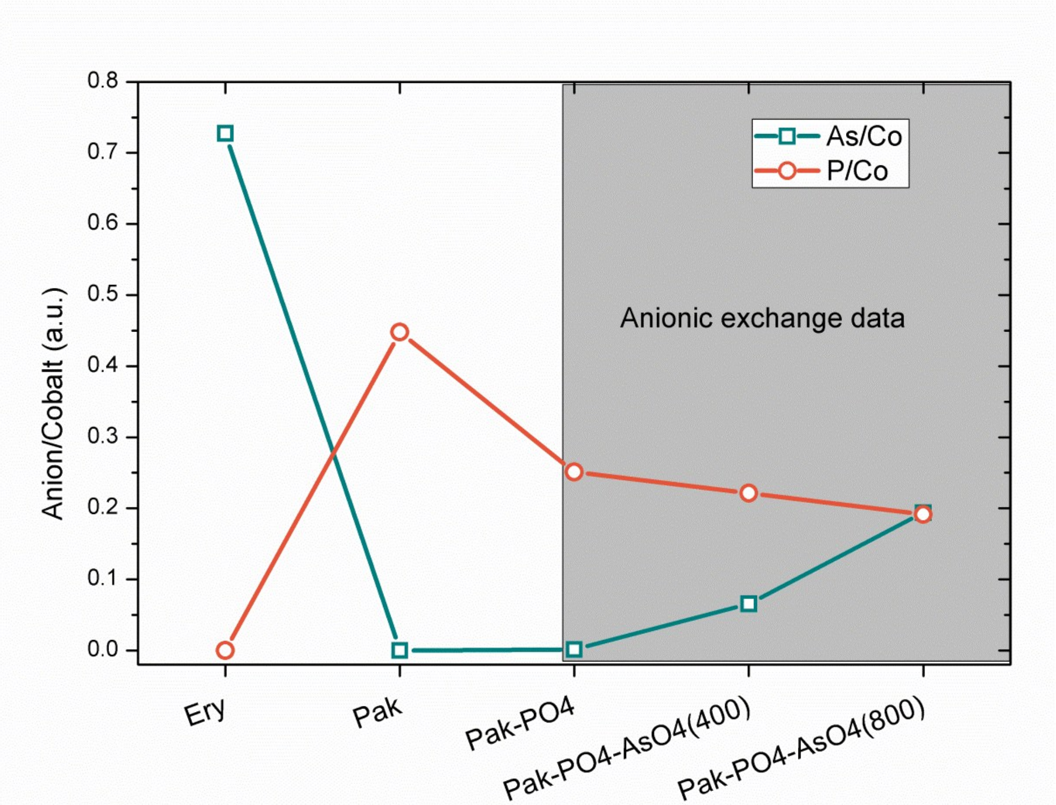

Figure S21. Anionic exchange study of pakhomovskyite first amorphized in 0.1 M and pH 7 phosphate buffer and then exchanged in 0.1 M and pH 7 arsenate buffer. The green line represents the mass proportion of arsenic in the sample normalized by the quantity of cobalt. The orange line represents the mass proportion of phosphorous in the sample normalized by the quantity of cobalt. **Ery**: Erythrite powder sample; **Pak**: pakhomovskyite powder sample; **Pak-PO4**: pakhomovskyite amorphized in 0.1 M and pH 7 phosphate buffer for 200 cycles 100 mVs^{-1}; **Pak-PO4-AsO4(400)**: pakhomovskyite amorphized in phosphate and anionic exchanged in arsenate buffer for 400 cycles at 100 mVs^{-1} (takes around 4 h); **Pak-PO4-AsO4(800)**: pakhomovskyite amorphized in phosphate and anionic exchanged in arsenate buffer for 800 cycles at 100 mVs^{-1} (takes around 8 h). The quantification of the different samples was performed by TXRF measurements using gallium as internal standard. It can be clearly observed how the proportion of arsenic increases in the film with the anionic exchange.

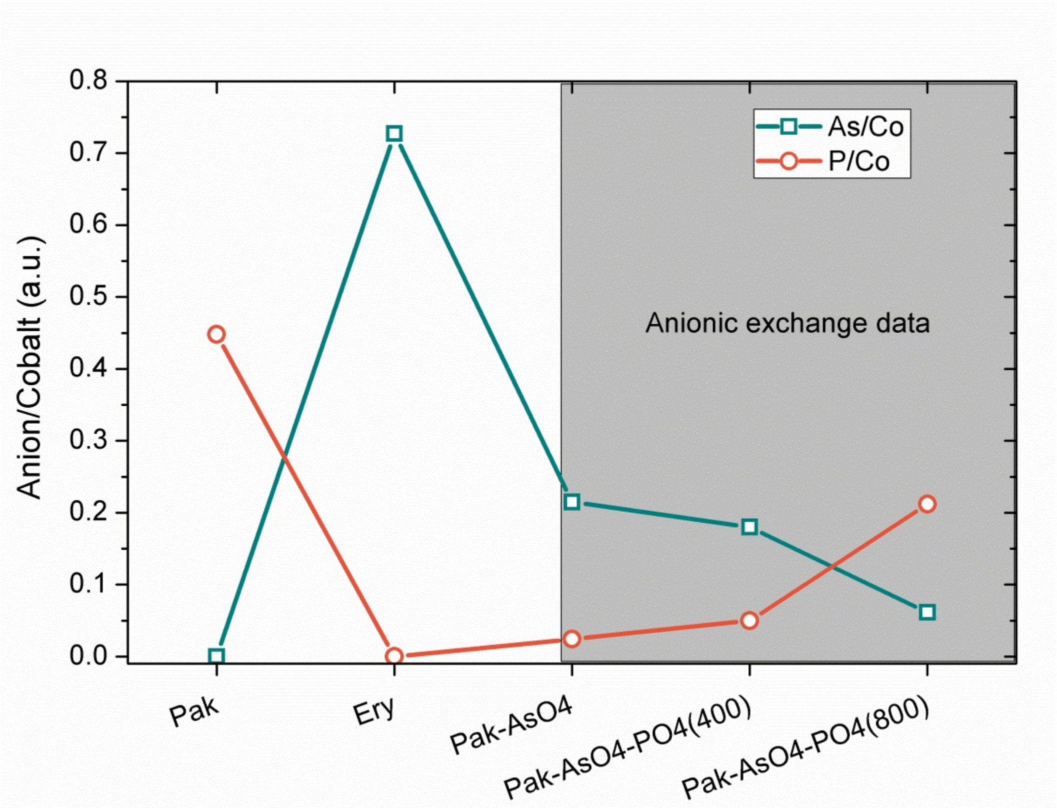

Figure S22. Anionic exchange study of pakhomovskyite first amorphized in 0.1 M and pH 7 arsenate buffer and then exchanged in 0.1 M and pH 7 phosphate buffer. The green line represents the mass proportion of arsenic in the sample normalized by the quantity of cobalt. The orange line represents the mass proportion of phosphorous in the sample normalized by the quantity of cobalt. **Ery**: Erythrite powder sample; **Pak**: pakhomovskyite powder sample; **Pak-AsO4**: pakhomovskyite amorphized in 0.1 M and pH 7 arsenate buffer for 200 cycles 100 mVs^{-1}; **Pak-AsO4-PO4(400)**: pakhomovskyite amorphized in arsenate and anionic exchanged in phosphate buffer for 400 cycles at 100 mVs^{-1} (takes around 4 h); **Pak-AsO4-PO4(800)**: pakhomovskyite amorphized in arsenate and anionic exchanged in phosphate buffer for 800 cycles at 100 mVs^{-1}(takes around 8 h). The quantification of the different samples was performed by TXRF measurements using gallium as internal standard. It can be observed how the initial proportion in the film is about 0.25 As/Co and is then decreased to almost 0 after 8 h exchange by phosphate.

Table S9. Quantification of the total amount of cobalt for the samples shown in Figure S21. The quantification was performed by TXRF. The electrodes had a geometric area of 1 cm^2.

Sample	Cobalt / $\mu g\ cm^{-2}$
Pak	30.125
Pak-PO_4	13.968
Pak-PO_4-AsO_4(400)	21.339
Pak-PO_4-AsO_4(800)	29.162

Table S10. Quantification of the total amount of cobalt for the samples shown in Figure S22. The quantification was performed by TXRF. The electrodes had a geometric area of 1 cm^2.

Sample	Cobalt / $\mu g\ cm^{-2}$
Pak	29.745
Pak-AsO_4	28.936
Pak-AsO_4-PO_4(400)	27.678
Pak-AsO_4-PO_4(800)	18.802

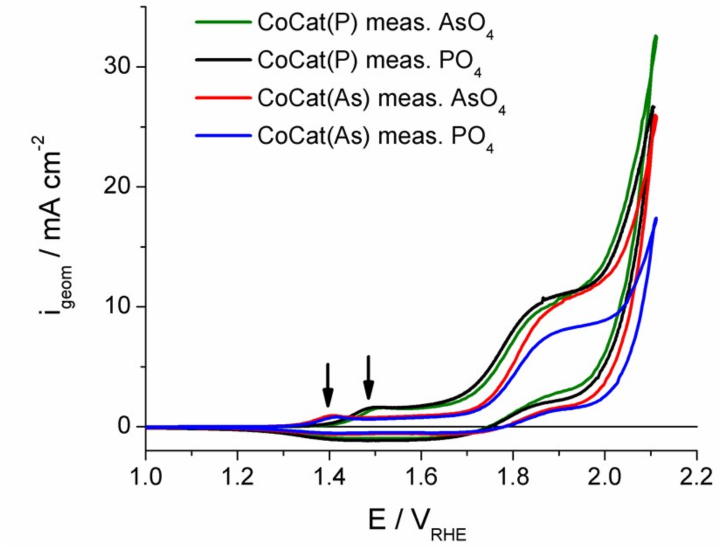

Figure S23. CV measurements for **CoCat(P)** (deposited in phosphate buffer 0.1 M and pH 7) and **CoCat(As)** (deposited in arsenate buffer 0.1 M and pH 7). Each type of sample was measured in 0.1 M and pH 7 phosphate buffer and in 0.1 M and pH 7 arsenate buffer, respectively. The CV measurements were performed at 100 mV s^{-1} scan rate and 85 % iR compensation.

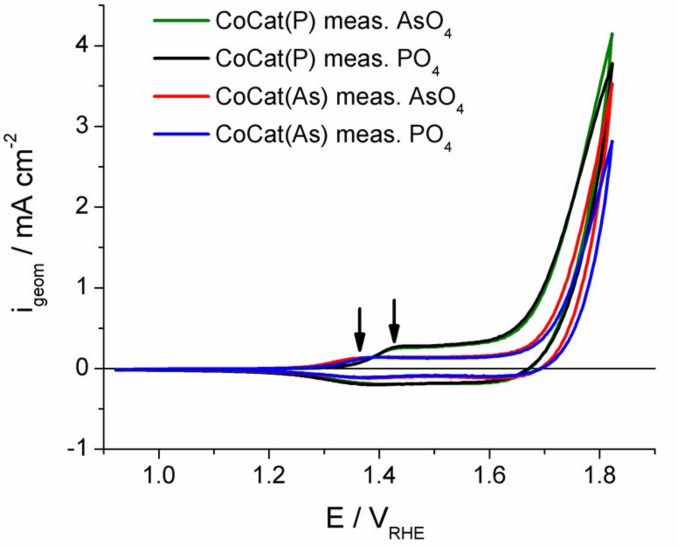

Figure S24. CV measurements for **CoCat(P)** (deposited in phosphate buffer 0.1 M and pH 7) and **CoCat(As)** (deposited in arsenate buffer 0.1 M and pH 7). Each type of sample was measured in 0.1 M and pH 7 phosphate buffer and in 0.1 M and pH 7 arsenate buffer, respectively. The CV measurements were taken at 20 mV s^{-1} scan rate and 85 % iR compensation.

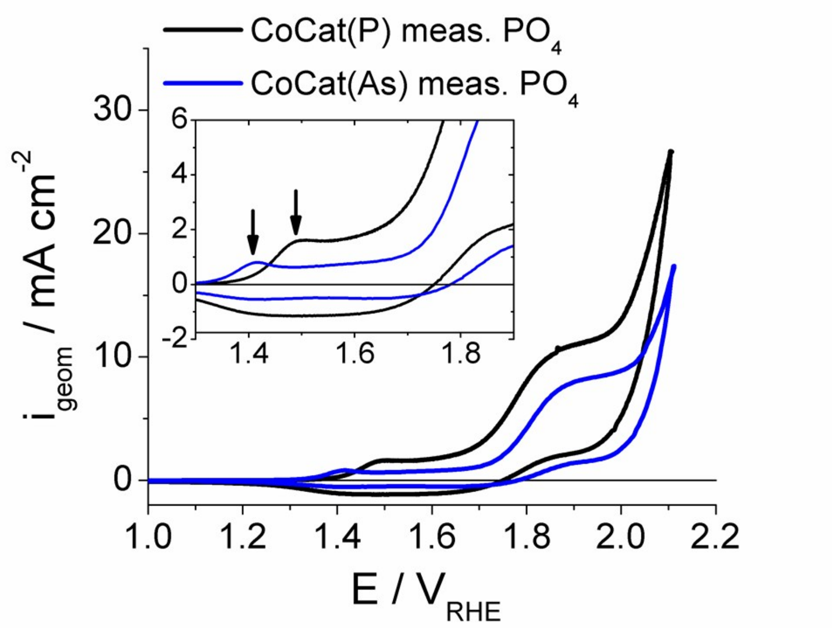

Figure S25. CVs measurements for CoCat(P) and CoCat(As) performed in 0.1 M and pH 7 phosphate buffer. The CVs were collected at 100 mV s^{-1} scan rate and 85 % iR compensation.

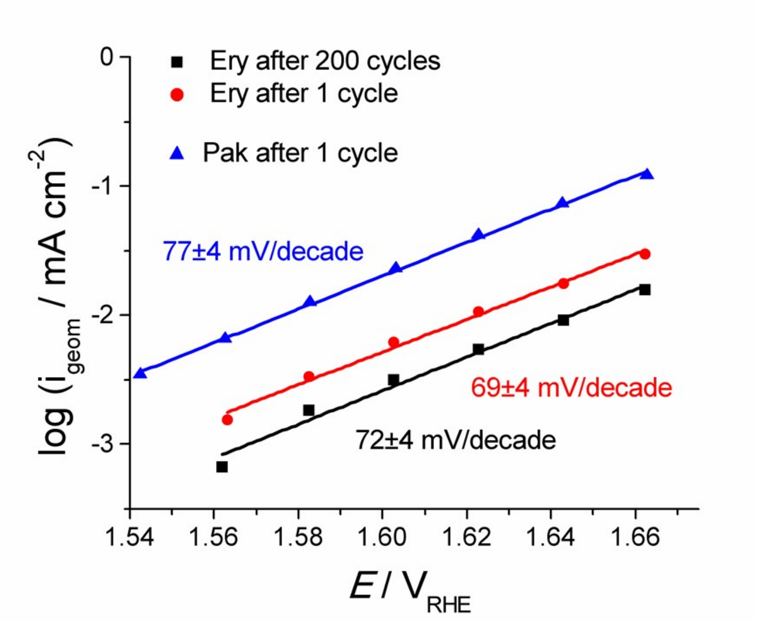

Figure S26. Tafel plots for pakhomovskyite (after the 1st CV cycle in 0.1 mol L^{-1} and pH 7 phosphate buffer) and erythrite (after the 1st and the 200th CV cycle respectively, in 0.1 mol L^{-1} and pH 7 phosphate buffer). The Tafel plots were measured with 100 mV steps with 5 min per step in phosphate buffer pH 7 and 0.1 mol L^{-1}.

Table S11. Comparison of Tafel slope values for in pakhomovskyite and erythrite before and after 200 cycles of amorphization in 0.1 M and pH 7 phosphate buffer.

Catalyst	Tafel Slope (mV/decade)	
	Before	After
Erythrite	69	72
Pakomovskite	77	73*

*Taken from reference [1].

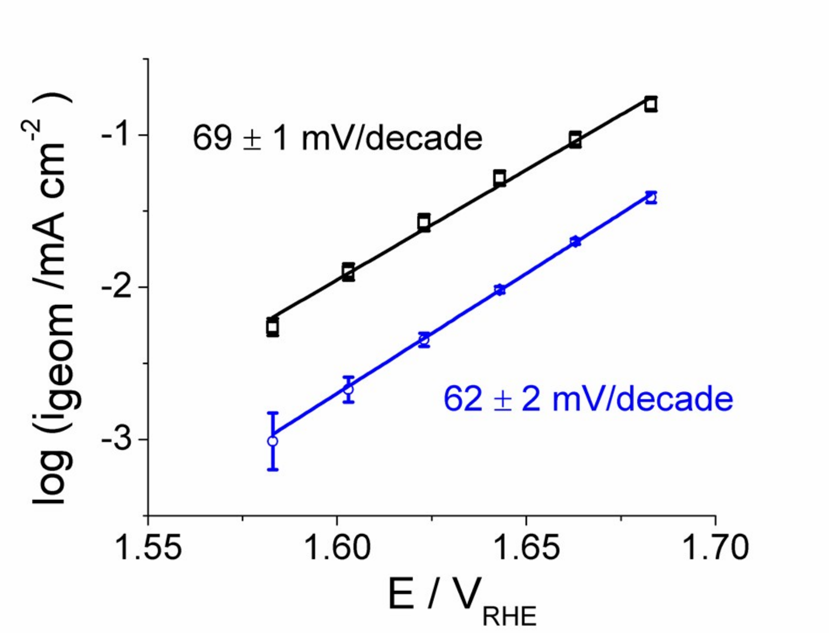

Figure S27. Tafel plots for **CoCat(P)** (deposited in phosphate buffer 0.1 M and pH 7) and **CoCat(As)** (deposited in arsenate buffer 0.1 M and pH 7). Each type of sample was measured in 0.1 M and pH 7 phosphate buffer. The Tafel plots were measured with 20 mV steps and 5 min per step. Each point corresponds to the average of 3 measurements.

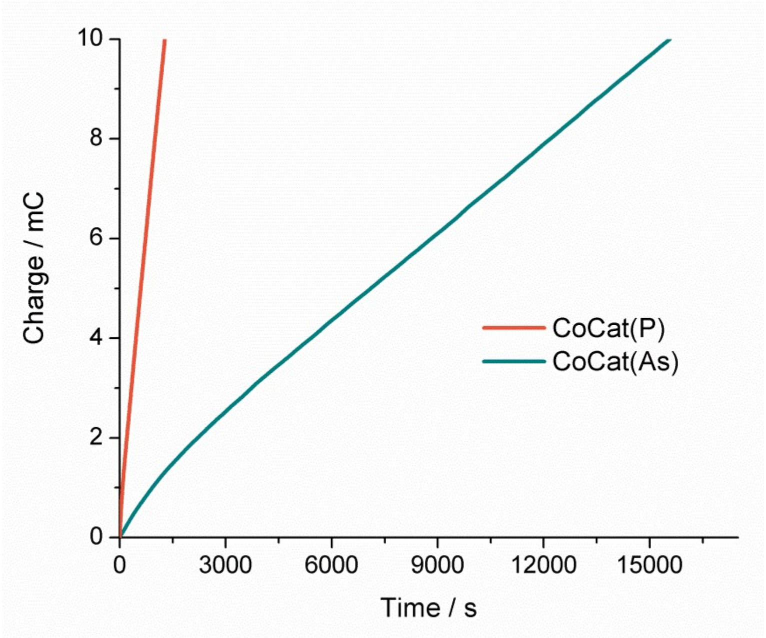

Figure S28. Deposition rate for CoCat(P) and CoCat(As). The deposition takes about 10 times longer for CoCat(As). The thickness of a 10 mC layer corresponds approximately to 70 nm according to the estimations by Klingan[4].

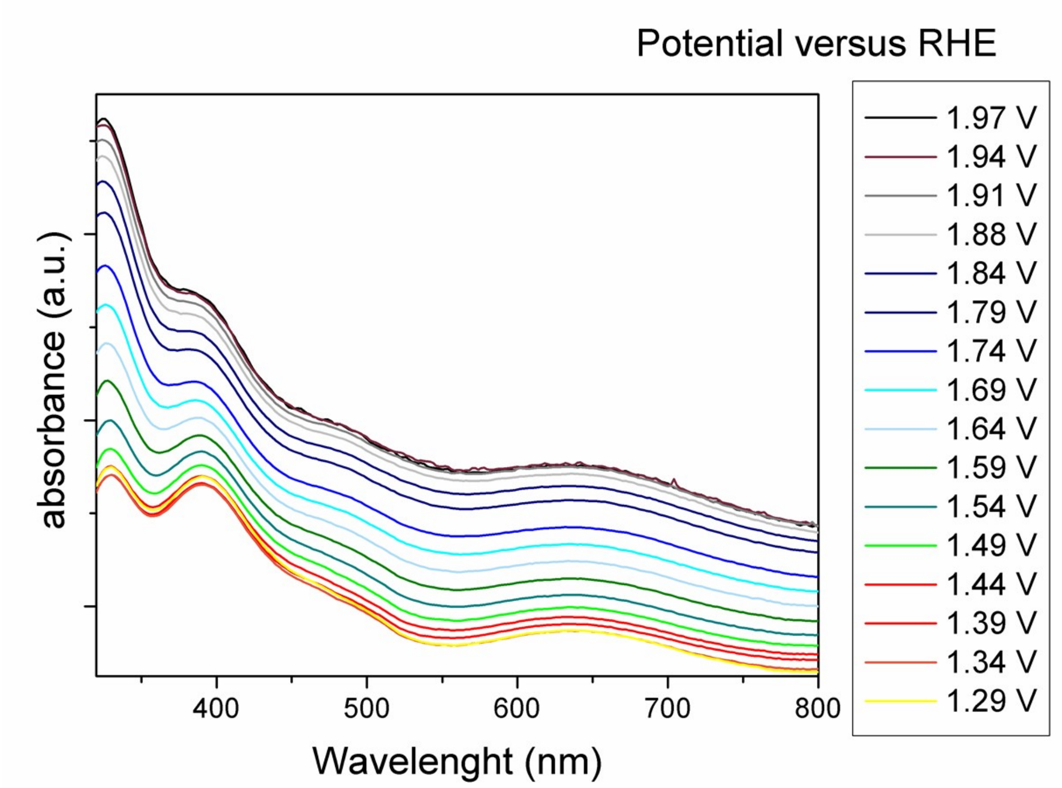

Figure S29. *In-situ* uv-vis absorption spectra of CoCat(P) films after equilibration for 2 min at the indicated electrode potential. All spectra were collected in 0.1 mol L^{-1} and pH 7 arsenate buffer; a clean FTO substrate was inserted into the spectro-electrochemical cell to record the baseline spectrum. Measurements were performed with a Lambda 1050 Spectrophotometer UV-VIS-NIR. The potential values are iR compensated, the Ohmic resistance was 42 Ω

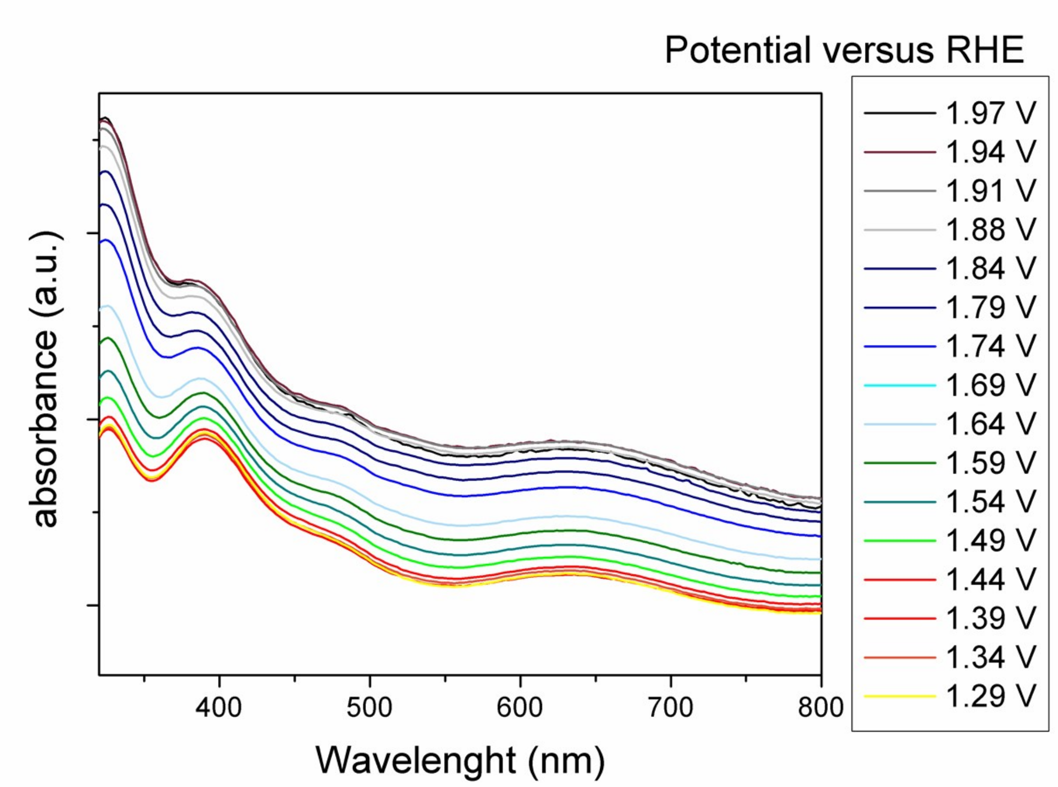

Figure S30. *In-situ* uv-vis absorption spectra of CoCat(As) films after equilibration for 2 min at the indicated electrode potential. All spectra were collected in 0.1 mol L^{-1} and pH 7 arsenate buffer; a clean FTO substrate was inserted into the spectro-electrochemical cell to record the baseline spectrum. Measurements were performed with a Lambda 1050 Spectrophotometer UV-VIS-NIR. The potential values are iR compensated, the Ohmic resistance was 42 Ω

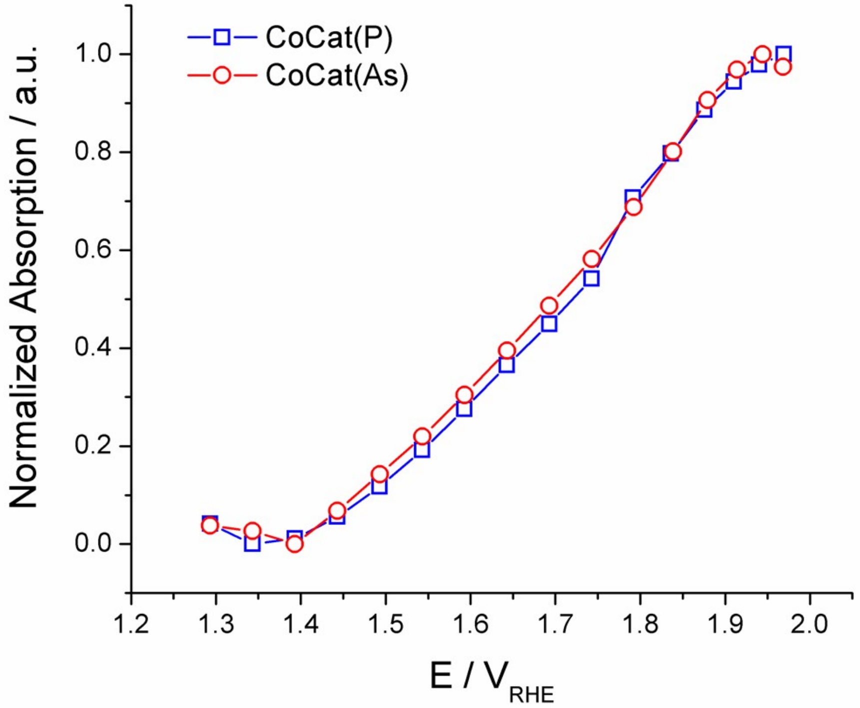

Figure S31. Changes in absorption at 420 nm for CoCat(As) and CoCat(P) for different applied potentials, obtained from *In-situ* uv-vis absorption measurements. Measurements were performed in 0.1 mol L^{-1} and pH 7 arsenate buffer. The potential values are iR compensated, the Ohmic resistance was 42 Ω in both cases.

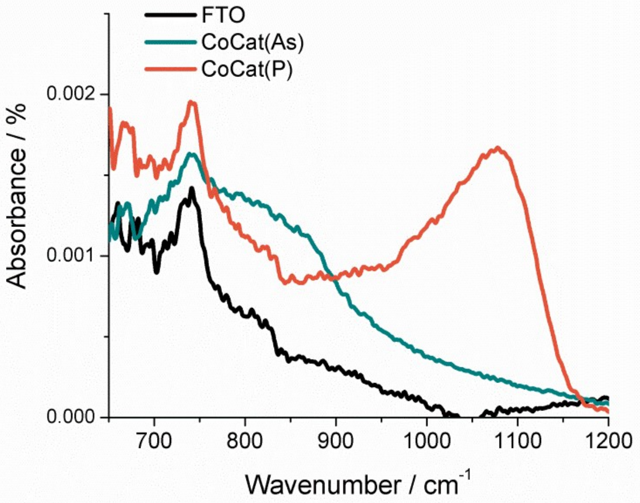

Figure S32. ATR-FTIR analysis for CoCat(P) and CoCat(As). Measurements were performed in a Thermo Scientific Nicolet 6700, in ATR mode using a diamond crystal.

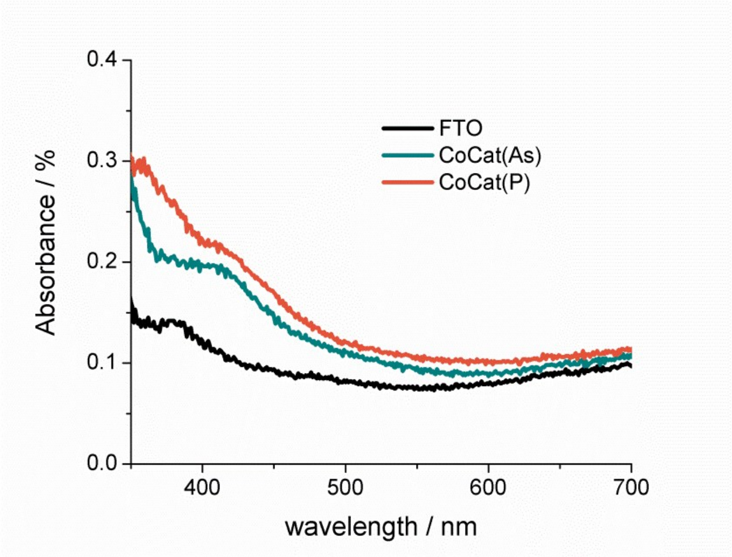

Figure S33. Uv-vis analysis for CoCat(P) and CoCat(As). Measurements were performed in a Thermo Scientific evolution 600 UV-visible with integration sphere (labsphere).

Bibliography

1 D. González-Flores, I. Sánchez, I. Zaharieva, K. Klingan, J. Heidkamp, P. Chernev, P. W. Menezes, M. Driess, H. Dau and M. L. Montero, *Angew. Chemie - Int. Ed.*, 2015, **54**, 2472–2476.
2 M. Risch, K. Klingan, F. Ringleb, P. Chernev, I. Zaharieva, A. Fischer and H. Dau, *ChemSusChem*, 2012, **5**, 542–549.
3 J. Mähler, R. Herbert and I. Persson, *Dalt. Trans.*, 2012, **42**, 1364–1377.
4 K. Klingan, F. Ringleb, I. Zaharieva, J. Heidkamp, P. Chernev, D. Gonzalez-Flores, M. Risch, A. Fischer and H. Dau, *ChemSusChem*, 2014, **7**, 1301–1310.